

Mapping of Geological Structures: A CNN Approach

Ayoub Fatihi¹ 

¹Institute of Earth Sciences, Faculty of Geosciences and Environment , University of Lausanne, Lausanne, Switzerland.

Keywords: CNN U-Net, deep learning, geological fractures, mapping

Abstract

Geological structures hold valuable information about the history of the Earth and earthquake mechanics. They are therefore critical when seeking resources such as water, petroleum, and minerals. Nowadays, a lot of data is obtained from drones and satellites, but extracting this information across multiple scales in a timely manner is a real challenge. Despite the efforts in recent years, the semi-automated processes still take a long time and need heavy input from researchers. Here we consider the use of deep learning-based methods which could enable a fully automatic workflow to map geological structures. Intentionally we trained a CNN with a data obtained from different datasets, each featuring a different scale. This CNN was then fine-tuned by exploring different parameters. Evaluations were conducted, shedding light on the efficacy, strengths, and limitations of this approach. This paper showcases the potential of deep neural networks for this task. We expect these methods to be a game changer in the way we map geological features from imagery.

Contents

| | | |
|---|--------------|---|
| 1 | Introduction | 1 |
| 2 | Data | 2 |
| 3 | Model | 3 |
| 4 | Results | 4 |
| 5 | Performance | 4 |
| 6 | Discussion | 5 |
| 7 | Conclusion | 5 |

1. Introduction

Within the Earth’s crust, fractures and faults are prevalent, and these geological features are associated with serious hazards, notably tectonic earthquakes, induced seismicity, landslides, and rock reservoir fracturing. Remote sensing datasets are commonly employed to study these geological features. These datasets, now regularly provided by satellites, aerial, and unmanned aerial vehicle (UAV) platforms, have reached a level of sophistication where they are readily accessible in high detail and are frequently updated. However the potential of these datasets is not fully exploited as the manual extraction of geological information from these data is no longer practical.

There has been significant efforts in recent years to develop semi-automatic and automatic methods for mapping structural data, but the task is challenging due to intrinsic variables such as geometry, soft linkage, and segmentation over multiple scales. And extrinsic variables, these include natural variations in colour, shadows, glare and/or incomplete geological exposure (Thiele et al., 2017).

In this paper we will use deep learning to automatically trace the structures in imagery datasets. Next we describe the implementation of this neural network and the choice of certain parameters.

2. Data

The data utilized in this research was collected from Mattéo et al.'s publication (2021). In three specific regions within the Granite Dells area, denoted as Sites A, B, and C (see Figure 1), a total of 165 RGB photos were captured from ground level using a standard optical camera (Panasonic Lumix GX80) positioned 3 meters above the ground (Mattéo et al., 2021). The ortho-images and DSMs for Sites A, B, and C were generated using Agisoft Metashape software with ultra-high resolutions (Mattéo et al., 2021). The ortho-images and DSMs are not geo-referenced (Mattéo et al., 2021).

2.1. Splitting data

The first law of geography states that nearer things are more related to each other than distant things. Randomly selecting assessment data may produce assessment sets that are not truly independent of data used to train the model. Hence, spatial cross-validation was chosen.

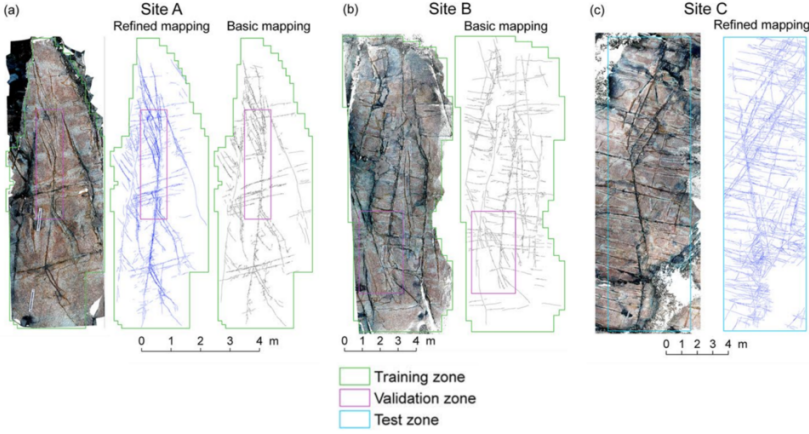


Figure 1: Sites, images, and ground truth fault maps (Mattéo et al., 2021). Training, validation and test zones are indicated in green, purple and blue, respectively.

2.2. Pre-processing

We formed a single band from the RGB bands using the approach in Equation Equation 1. Subsequently, we applied the contrast-limited adaptive histogram equalization (CLAHE) technique, guided by the methodology outlined in HatiPoglu et al., 2022. Various experiments were conducted with different settings to determine the optimal parameter values.

$$B_5 = \frac{R + 2 \cdot G + B}{4} \quad (1)$$

2.3. Data augmentation

To enhance the efficacy of our model, we utilized data augmentation methodologies throughout the training phase. This augmentation encompassed the application of various transformations to the initial images, thereby instilling diversity and variability into the dataset. Concretely, we integrated rotations within a 0.2-degree range, horizontal and vertical shifts within a 0.05-pixel range, shearing within a

0.05 range, zooming within a 0.05 range, and horizontal flipping. Furthermore, we configured the fill mode to 'nearest' to rectify any potential lacunae or voids arising during the augmentation procedure.

3. Model

3.1. Exploration

Multiple variants of data were experimented with:

1. RGB channels
2. RGBA (alpha channel representing the output of the CLAHE pre-processing)
3. RGBA (alpha channel representing topography/altitude)

Next, we will share the best-performing combination (3) utilizing the U-Net architecture.

3.2. U-Net

The U-Net architecture comprises an encoder and a decoder, featuring convolutional layers instead of fully connected layers. This configuration is employed to transform input images into binary image maps. Figure 2 depicts the chosen architecture.

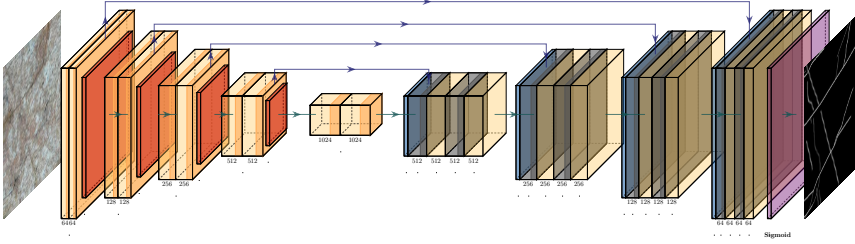


Figure 2: Architecture of U-Net CNN (U-Net-0)

3.2.1. Loss function

Our goal is to create a binary image where each pixel is given a probability value to indicate if it belongs to the fractures category or not. However, the significant class imbalance in the ground truth images presents a challenge, with about 99.7% of pixels representing the background and only a small fraction corresponding to fractures. Training a neural network under these conditions can be challenging, as it may converge towards local minima and become biased towards the dominant background class.

To effectively tackle this issue, we suggest incorporating the dice function (Milletari et al., 2016) as a loss function in the training process to optimize the network's parameters. The dice loss function, known for its differentiable approximation, proves beneficial in addressing class imbalance.

The dice loss formula, as shown in Equation 2, provides a practical solution for handling challenges related to unbalanced training data. Importantly, it eliminates the need to specify weighting parameters between different classes, like background and fractures, during training. This characteristic makes the dice loss function well-suited for binary segmentation tasks.

$$L_{dice} = 1 - \frac{2 \sum_{x \in \Omega} p_l(x) g_l(x)}{\sum_{x \in \Omega} p_l^2(x) + \sum_{x \in \Omega} g_l^2(x)} \quad (2)$$

Here, $p_l(x)$ denotes the probability of pixel x belonging to class l , and $g_l(x)$ is a vector representing the ground truth label, with a value of one for the true class and zero for other classes.

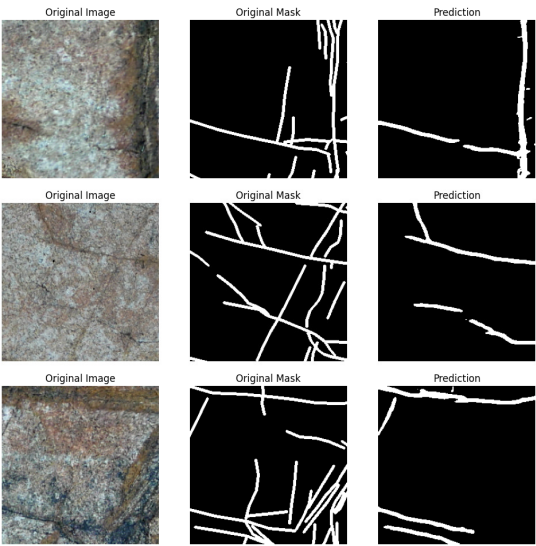


Figure 3: Results of the U-Net model (08)

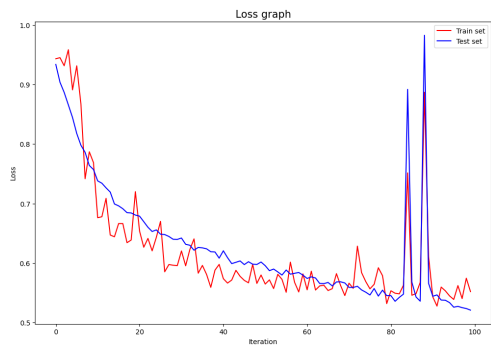


Figure 4: Loss graph

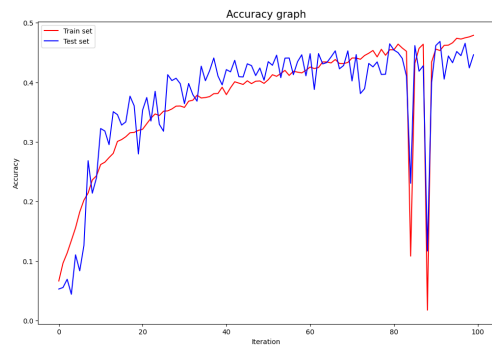


Figure 5: Accuracy graph

Table 1: Performance metrics on test data

| Model | Loss (Dice Loss) | Binary Accuracy | IoU | Dice Coeff. | AUC |
|-------|------------------|-----------------|------|-------------|------|
| U-Net | 0.64 | 0.95 | 0.22 | 0.36 | 0.64 |

4. Results

In this section, we present the outcomes of our proposed method. Figure 3 illustrates the original masks alongside predictions generated by the model for comparative analysis.

5. Performance

Figure 4 illustrates the evolution of the loss function throughout the training period. Additionally, Table 1 provides the performance metrics on the test data.

6. Discussion

Data needs verification; exemplified in Figure 6, as it appears the labeling may be incorrect, compromising data quality. Additionally, an investigation is required to analyze the two spikes observed in the loss and accuracy graphs.

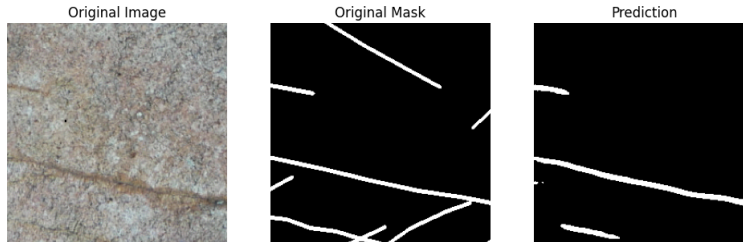


Figure 6: Can we rely on the quality of this data?

7. Conclusion

The findings are quite exciting, suggesting that deep learning can be useful for mapping geological structures. To make progress, we must start by defining the problem and creating a solid architecture for effective training. There's still much work ahead, including obtaining high-quality data and making the model adaptable. Future research should tackle challenges like imbalanced data, refining transfer learning capabilities, and improving the overall efficiency of the process.

Data Availability

The repository <http://doi.org/10.5281/zenodo.4611494> provides access to the images and topographic data as well as the ground truths utilized for training, validation, and testing as .tif files (Mattéo et al., 2021).

Code

The code is available at the following link: <https://github.com/ayoubft/frac-map-dl>.

Acknowledgements

I extend my sincere gratitude to Professor Tom Beucler and the Teaching Assistants for their efforts in the course (Machine Learning for Earth and Environmental Sciences 2023), as well as for providing constructive feedback.

References

- HatiPoglu, B., Karagoz, I., & INal, M. (2022). Threshold Based Image Enhancement Method for Low Contrast X-Ray Images Using CLAHE. *Uluslararası Muhendislik Arastirma ve Gelistirme Dergisi*. <https://doi.org/10.29137/umagd.1203617>
- Mattéo, L., Manighetti, I., Tarabalka, Y., Gaucel, J.-M., van den Ende, M., Mercier, A., Tasar, O., Girard, N., Leclerc, F., Giampetro, T., Dominguez, S., & Malavieille, J. (2021). Automatic Fault Mapping in Remote Optical Images and Topographic Data With Deep Learning. *Journal of Geophysical Research: Solid Earth*, 126(4), e2020JB021269. <https://doi.org/10.1029/2020JB021269>
- Milletari, F., Navab, N., & Ahmadi, S.-A. (2016, June). V-Net: Fully Convolutional Neural Networks for Volumetric Medical Image Segmentation. <https://doi.org/10.48550/arXiv.1606.04797>
- Thiele, S. T., Grose, L., Samsu, A., Micklethwaite, S., Vollgger, S. A., & Cruden, A. R. (2017). Rapid, semi-automatic fracture and contact mapping for point clouds, images and geophysical data. *Solid Earth*, 8(6), 1241–1253. <https://doi.org/10.5194/se-8-1241-2017>